Key Words:
DWPF, hydrogen
Noble metals
Acid usage

Retention:
Permanent

SLUDGE CHARACTERIZATION AND SRAT SIMULATIONS USING A NITRITE-FREE SLUDGE SIMULANT

D. C. Koopman

DECEMBER 2009

Savannah River National Laboratory
Savannah River Nuclear Solutions
Aiken, SC 29808

Prepared for the U.S. Department of Energy Under
Contract Number DE-AC09-08SR22470

SRNL
SAVANNAH RIVER NATIONAL LABORATORY

DISCLAIMER

Printed in the United States of America

Prepared for
U.S. Department of Energy

Key Words:
DWPF, Noble Metals, H_2, Acid Usage

Retention:
Permanent

SLUDGE CHARACTERIZATION AND SRAT SIMULATIONS USING A NITRITE-FREE SLUDGE SIMULANT

D. C. Koopman

DECEMBER 2009

Savannah River National Laboratory
Savannah River Nuclear Solutions
Savannah River Site
Aiken, SC 29808

Prepared for the U.S. Department of Energy Under Contract Number DE-AC09-08SR22470

SRNL SAVANNAH RIVER NATIONAL LABORATORY

REVIEWS AND APPROVALS

D. C. Koopman, Process Technology Programs Date

M. E. Stone, Peer Reviewer, Process Technology Programs Date

C. C. Herman, Manager, Process Technology Programs Date

S. L. Marra, Manager, Date
Environmental & Chemical Process Technology Research Programs

J. E. Occhipinti, Manager Date
Waste Solidification Engineering

TABLE OF CONTENTS

LIST OF FIGURES

LIST OF TABLES

LIST OF ACRONYMS

ACTL	Aiken County Technology Laboratory
AD	Analytical Development
CPC	Chemical Process Cell
CSTR	Continuous Stirred Tank Reactor
DWPF	Defense Waste Processing Facility
E&CPT	Environmental and Chemical Process Technology
FAVC	Formic Acid Vent Condenser
GC	Gas Chromatograph
IC	Ion Chromatography
ICP-AES	Inductively Coupled Plasma-Atomic Emission Spectroscopy
ICP-MS	Inductively Coupled Plasma-Mass Spectroscopy
LWO	Liquid Waste Organization
MWWT	Mercury Water Wash Tank
NFT	Nitrite free test
PSAL	Process Science Analytical Laboratory
QA	Quality Assurance
SB	Sludge Batch
SCFM	Standard Cubic Feet per Minute
SME	Slurry Mix Evaporator
SRAT	Sludge Receipt and Adjustment Tank
SRNL	Savannah River National Laboratory
SRNS	Savannah River Nuclear Solutions
SRR	Savannah River Remediation
STI	Scientific and Technical Information
TA	Technical Analyst
TIC	Total Inorganic Carbon
TR	Technical Report

1.0 EXECUTIVE SUMMARY

Understanding catalytic hydrogen generation is fundamental to the safe operation of the Defense Waste Processing Facility (DWPF) Chemical Process Cell (CPC). Two Sludge Receipt and Adjustment Tank (SRAT) simulations were completed at the Aiken County Technology Laboratory (ACTL) of the Savannah River National Laboratory (SRNL) using a nitrite-free starting simulant. One simulation was trimmed with Rh and Hg and the other with Ru and Hg. The two noble metals were trimmed at the upper end of the recent Rh-Ru-Hg study. Mercury was trimmed at 1.5 wt% in the total solids. Excess acid comparable in quantity to that in the recent Rh-Ru-Hg matrix study was used. In spite of the favorable conditions for hydrogen generation, virtually no hydrogen production was observed during either SRAT simulation.

The Rh test result confirmed the postulated significance of nitrite ion to the catalytic reactions producing hydrogen in CPC testing with normal DWPF sludge simulants. As for Ru, however, previous testing has shown that Ru activated for hydrogen generation only after nitrite destruction. Therefore, Ru could have potentially been catalytically active from the start of the nitrite-free SRAT test, but no such activity was seen. The nitrite-free Ru test result suggests that the intermediate form detected in the bead-frit melter feed preparation Ru solubility profiles was some form of nitro-Ru complex. The nitro-Ru complex is apparently not catalytically active for hydrogen generation but is a precursor to the catalytically active form (presumably a different complex not involving nitrite ligands). Removing nitrite ion from the system prevented the Ru catalyst precursor from forming and consequently blocked formation of the catalytically active form.

These results, along with the results of a simulation in which sodium nitrite was metered into the SRAT to prevent ligand substitution reactions that occur during nitrite destruction from occurring in order to reduce hydrogen generation, have greatly clarified the role of the nitrite ion in SRAT hydrogen generation. The new findings add to the overall fundamental understanding of catalytic hydrogen generation during waste processing in the DWPF. These findings also address one of the issues raised in the Future Work section of the recent summary document concerning catalytic hydrogen generation in the CPC.[1] The knowledge gained should facilitate planning future experiments.

2.0 INTRODUCTION

SRNL has been researching the chemistry of catalytic hydrogen generation in the DWPF CPC. This program has identified Rh, Ru, nitrite ion, Hg, and excess acid as the five principal factors. These conclusions were presented in a recent status summary report, which includes references that lead to most relevant prior work on the subject.[1] The maximum hydrogen generation rate in the SRAT often occurred near the end of nitrite destruction and was correlated with the Rh concentration. Some simulations, however, had a greater maximum hydrogen generation rate occur after nitrite destruction which was due to a catalytic contribution from Ru that exceeded the maximum hydrogen generation rate due to Rh.

Nitrite was found to have an impact on both Rh and Ru catalysis. Rh was active in converting nitrite to N_2O when nitrite concentrations were greatly in excess of the Rh concentration. Destruction of all of the remaining available nitrite seemed to be associated with deactivation of the principal Rh catalyst. Conversely, Ru appeared to be nearly inactive at high nitrite ion concentrations. Ru would activate for hydrogen generation only after nitrite ion concentrations were reduced to comparable or lower levels than the Ru concentration. Mercury, which generally inhibited catalytic hydrogen generation to some extent in direct comparison SRAT simulations with and without mercury, was found to catalyze the reductive conversion of nitrite to NO and CO_2 by formic acid. Altering the rate of nitrite destruction will change the timing of catalytic hydrogen generation by both Rh and Ru.

The analysis of the experimental data led to a few questions that were included as areas for future work in the status summary report:[1]

First, Ru seemed to go through a transitional form based on solubility data before the catalytically active form for hydrogen generation appeared. The identity of both forms remains unknown. Literature data suggests that Ru-carbonyl complexes may be one candidate for the hydrogen catalyst. Absorbed CO_2 from decomposition of formic acid may be the key to forming such complexes, since the initial carbonate in the sludge is typically consumed several hours before Ru becomes active.

Second, how much of the inferred Rh and Ru hydrogen catalysis control by nitrite ion is actually due to the changing background concentration of nitrite? Would hydrogen generation occur in the absence of nitrite altogether? Sodium nitrite solution was metered into an earlier SRAT simulation once GC data indicated that the catalyst(s) had become active for hydrogen. This strategy was successful in partially suppressing hydrogen generation, and it showed the potential to be even more effective with an improved $NaNO_2$ addition strategy.

Third, why does mercury inhibit catalysis in head-to-head tests performed with and without mercury present and everything else equal? The more detailed analysis so far has only found Hg to be important at altering the timing of nitrite destruction. In addition, even small

amounts of Hg in the starting sludge (~0.1 wt% in total solids) cause significant changes in hydrogen generation compared to identical sludges without mercury. Changing the timing of hydrogen generation through altered nitrite destruction kinetics has the potential to either increase or decrease the maximum hydrogen generation rate (increase by aligning the most active catalyst form with a greater quantity of excess acid). Investigations targeted to determine what is different between a simulant without mercury and one with a low concentration of mercury are not planned, since there are no mercury-free waste sludges to feed DWPF in the SRS tank farm (the question is apparently hypothetical except for special simulant sludge tests and in the preparation of mercury-free melter feed simulants).

Progress on the first two questions above was thought to be possible if a simulant could be prepared that was nitrite-free. The Sludge Batch 6 parametric simulant properties study had produced some unwashed, untrimmed simulant during transitions in the precipitation vessel conditions. This excess simulant was nitrite-free. A portion of this simulant was taken, washed, and trimmed to supernate concentrations similar to recent SRAT tests in the hydrogen generation program (except for the absence of nitrite). This nitrite-free simulant was used to perform two SRAT simulations. One SRAT was trimmed with rhodium nitrate solution and HgO. The other was trimmed with soluble $RuCl_3$ and HgO. It was hypothesized that the Rh test might produce very minimal hydrogen, since the nitro-Rh complexes would not form in the absence of nitrite (unless some nitrate ions were to convert to nitrite ions). It was further hypothesized that the Ru test might produce significant hydrogen, and that this hydrogen might be seen earlier than normal (for Ru), due to the absence of the inhibiting nitrite ion. This report summarizes the preparation of the nitrite-free simulant and the results obtained performing these two nitrite-free SRAT simulations.

3.0 APPROACH

3.1 PROCESS AND SAMPLE ANALYTICAL METHODS

The automated data acquisition system developed for the 4-L SRAT rigs was used to collect electronic data. Collected data included SRAT temperature, bath temperatures for the cooling water to the SRAT condenser and Formic Acid Vent Condenser (FAVC), slurry pH, SRAT mixer speed and torque, air and helium purge flows (He is used as an internal standard and is set to 0.5% of the nominal SRAT air purge flow). Cumulative acid addition volume data were collected from the automated dispensers. Both tests had a pH probe in the SRAT slurry to monitor pH. Raw GC data were acquired on separate computers dedicated to each instrument.

Agilent 3000A micro GC's were used on both runs. The GC's were baked out before runs. Column-A can collect data related to He, H_2, O_2, N_2, NO, and CO, while column-B can collect data related to CO_2 and N_2O (and sometimes water). GC's were calibrated with a standard gas containing 0.499 vol% He, 1.000 vol% H_2, 20.00 vol% O_2, 51.0 vol% N_2, 25.0 vol% CO_2 and 2.50 vol% N_2O. Room air was used to give a two point calibration for N_2. The GC's were checked with calibration gas before and after the SRAT cycle.

The chilled off-gas leaving the FAVC was passed through a Nafion dryer in counter-current flow with a dried air stream to reduce the moisture content at the GC inlet. A fairly short unit was selected to minimize pressure drop, but it appears to be possible to significantly reduce the moisture content in the stream being sampled by the GC. The inlet GC samples also passed through small sintered metal filters prior to injection into the two columns. The dryer and filter are part of a program to extend GC service life.

Process samples were analyzed by various methods. Slurry and supernate elemental compositions were determined for the simulant and two SRAT products by inductively coupled plasma-atomic emission spectroscopy (ICP-AES) at the Process Science Analytical Laboratory (PSAL). Slurry samples were calcined at 1100°C, however, so noble metals, Pb, and Cr were underreported. Total slurry noble metal concentrations were determined using mass balance information. Soluble slurry anions were determined by ion chromatography (IC) on 100-fold weighted dilutions of slurry with water after filtering out insoluble solids. Starting simulant was submitted to Analytical Development (AD) for total inorganic carbon (TIC) analysis of both the total slurry and the supernate. Starting sludge and SRAT products were analyzed for slurry and supernate density using the Anton-Parr instrument at ACTL. Starting sludge was titrated to pH 7 using the ACTL auto-titrator to determine the base equivalents for input into the stoichiometric acid equation.

3.2 SIMULANT PREPARATION AND CHARACTERIZATION

A somewhat unique simulant was prepared for this study. The CSTR precipitator parametric study produced a fairly wide range of compositions due to the range of precipitation pH values that were studied. Some of these were very low in aluminum and very high in

manganese. The recipe basis was that for the Sludge Batch 6 (SB6) nominal washed case in the preliminary flowsheet study (SB6-A simulant).[2] The actual composition, was, however, quite different from that of the preliminary SB6 simulant.

Table 1 presents the average elemental analytical results from duplicate analyses of sample of the simulant. The sample was calcined at 1100° C followed by digestion for slurry elemental analysis.

Table 1. Simulant calcined (1100 °C) elemental composition, wt%

Element	Nitrite-free Simulant
Al	6.54
Ba	0.208
Ca	3.31
Ce	0.306
Cr	0.291
Cu	0.132
Fe	24.1
K	<0.10
La	0.147
Mg	2.01
Mn	9.65
Na	11.7
Ni	5.26
P	<0.10
Pb	0.047
S	0.376
Si	0.564
Sn	0.021
Ti	0.038
Zn	0.148
Zr	0.218

Table 2 gives wt% solids, density, titration, anion and inorganic carbon data for the nitrite-free simulant along with comparable results for the hydrogen program simulant used in most of the 2006-2008 catalytic hydrogen program testing. The key input parameters for stoichiometric acid equation calculations are included in Table 2.

Table 2. Other nitrite-free simulant analyses

	Nitrite-free Simulant	H_2 Program Simulant
Total solids, wt%	15.2	22.8
Insoluble solids, wt%	10.8	16.8
Soluble solids, wt%	4.4	6.0
Calcined solids, wt%	11.4	16.0
Slurry density, g/mL	1.10	1.18
Supernate density, g/mL	1.04	1.05
Slurry base equiv., mol/kg	0.539	0.313
Nitrite, mg/kg	<100	17,900
Nitrate, mg/kg	15,200	13,800
Sulfate, mg/kg	1,100	1,600
Oxalate, mg/kg	<100	1,400
Chloride, mg/kg	188	390
Slurry TIC, mg/kg	732	1430
Supernate TIC, mg/kg	360	660

The nitrite-free simulant was considerably more viscous than the hydrogen program simulant. Consequently, it was impractical to increase the wt% total solids of the nitrite-free simulant to match those of the hydrogen program simulant. Both nitrite-free simulant SRAT tests had 3,000 g of starting sludge (before trim chemicals and rinse water). Rh was trimmed as a 4.93 wt% rhodium solution of $Rh(NO_3)_3$. Ru was added as the dry trivalent chloride salt at a purity of 41.73 wt% Ru. Mercury was trimmed as dry HgO.

The noble metal targets for the two nitrite-free simulant tests were matched to the high end concentrations in the Rh-Ru-Hg matrix study.[3] These concentrations are 5/3rd the mid-point concentrations in that study. This choice offset the fact that the total solids concentration was only about 2/3rd as high (~2/3*5/3 ≈ 1). Therefore, the noble metal concentrations in the nitrite-free SRAT simulations were comparable to the midpoint concentrations in the Rh-Ru-Hg matrix study on a slurry basis (mg noble metal/kg slurry). The two nitrite-free tests, NFT1 and NFT2, mercury and noble metal targets are given in Table 3 as wt% in the total solids of the trimmed slurry along with two comparison cases from the Rh-Ru-Hg matrix study, the midpoint case and the high Rh-high Ru-low Hg case, H-H-L. Silver and palladium were excluded from the two nitrite-free SRAT simulations to eliminate any potential confounding effects on the results.

Table 3. Noble metal and mercury targets, wt% in total solids

	Ag	Pd	Rh	Ru	Hg
Rh-Ru-Hg midpoint	0.0010	0.0003	0.0078	0.0300	1.500
Rh-Ru-Hg H-H-L	0.0010	0.0003	0.0130	0.0500	0.500
NFT1	0	0	0.0131	0	1.500
NFT2	0	0	0	0.0505	1.500

The slurry concentrations of the noble metals and mercury are given in Table 4.

Table 4. Noble metal and mercury targets, mg/kg slurry

	Ag	Pd	Rh	Ru	Hg
RhRuHg midpoint	2.3	0.7	18	68	3420
RhRuHg H-H-L	2.3	0.7	30	114	1140
NFT1	0	0	20	0	2280
NFT2	0	0	0	77	2280

3.3 CHEMICAL PROCESS CELL SIMULATION DETAILS

The trimmed SRAT receipt volume was about 2.6 L. The amount of acid to add was not determined by selecting an arbitrary stoichiometric factor. The stoichiometric acid requirement of the hydrogen program simulant and the nitrite-free simulant were determined using the new Koopman minimum acid requirement equation:[4]

$$\frac{moles\ acid}{L\ slurry} = base\ equivalents + Hg + soluble\ TIC + 1.5*(Ca + Mg) + 1.0*nitrite + 1.5*Mn$$

The amount of acid used in the Rh-Ru-Hg matrix study SRAT simulations above the Koopman minimum acid calculation value was determined by difference to be about 0.61 moles acid/L SRAT receipt slurry. That incremental quantity of additional acid was added to the stoichiometric requirement determined for the nitrite-free simulant to obtain the total acid addition for the SRAT simulations. The results of these calculations are summarized in Table 5.

Table 5. Stoichiometric acid calculation results, moles acid/L slurry

	Min. Koopman moles/L	Actual moles/L	Stoichiometric factor
Rh-Ru-Hg	1.41	2.02	143%
Nitrite-free	1.22	1.83	150%

The higher base equivalents of the nitrite-free simulant partially off-set the absence of nitrite, as did the higher Mn concentration. The net result was that the stoichiometric factor only changed from 143% to 150%. The essential goal was to ensure that there was a reasonable quantity of excess acid available in the two nitrite-free tests for producing hydrogen should either noble metal become catalytically active at levels comparable to normal SRAT simulations. Constraining this goal was the desire to not create a potential situation where hydrogen generation would greatly exceed the equivalent to the DWPF design basis limit of 0.65 lbs H_2/hr in the off-gas system.

Total acid was partitioned between formic and nitric acids using the latest RedOx equation.[5] An assumption of 20% formate loss was also made to enable this calculation to be performed

without any prior experience with these simulants. As a result, formic acid made up 94.5% of the total acid.

Nominal scaled DWPF SRAT processing conditions were generally used. The SRAT cycle, however, did not have a heel from a prior batch.

- The SRAT air purge scaled to 230 scfm in DWPF.
- A 200 ppm antifoam addition was made prior to nitric acid addition.
- A 100 ppm antifoam addition was made prior to formic acid addition.
- Nitric and formic acid addition were made at 93°C.
- Acid was added at two gallons per minute scaled from 6,000 gallons to 2.6 L.
- A 500 ppm antifoam addition was made prior to going to boiling following acid addition.
- Boiling assumed a condensate production rate of 5,000 lbs/hr at DWPF scale.
- SRAT dewatering was performed to adjust the slurry volume and meet the SRAT total solids target (about 80-90 minutes).
- Reflux followed dewatering. The end of a 12-hour reflux period defined the end of the SRAT cycle. It was projected that mercury might exceed the DWPF SRAT product limit after only 13-14 total hours at boiling due to the high initial concentration. This was not relevant to this particular study which was focused on catalytic hydrogen generation.

The SRAT product slurry was sampled directly into a digestion bottle while mixing once it had cooled to 90 °C. These samples were for possible mercury analysis. The remaining SRAT product samples were taken after the product had cooled and been weighed. The MWWT and FAVC were drained and weighed. A complete SRAT simulation took about 21 hours measured from the start of heating prior to acid addition in the SRAT until the time that the SRAT product had cooled to less than 50 °C.

4.0 SRAT SIMULATION RESULTS

This section discusses the processing and analytical data obtained from the two nitrite-free SRAT simulations.

4.1 ANION COMPOSITION CHANGES

SRAT product samples were taken and analyzed for elements, anions, solids, etc. These samples were taken once the SRAT had cooled to below 50 °C. Results are presented for the anions and the slurry pH in Table 6. The end of reflux pH is from the pH probe in the SRAT vessel at about 101 °C, while the SRAT product sample pH is from a separate analytical probe used by PSAL on room temperature samples.

Table 6. Anion concentration, mg/kg, end of SRAT cycle

	NFT1-Rh	NFT2-Ru
Nitrite ion – product	<100	<100
Formate ion – product	66,700	66,600
Nitrate ion – product	23,300	23,500
Sulfate ion – product	150	<100
SRAT pH, end of reflux	4.22	4.18
SRAT product sample pH	4.71	4.79

Nearly identical results were obtained for the two SRAT products. The similarity was consistent with the identical acid additions and general lack of catalytic activity observed.

Anion data were combined with material balance data. The resulting calculations were used to determine the formate loss. The pre-run acid calculations were prepared assuming 20% formate loss. The results of these calculations are given in Table 7 along with the calculated RedOx state as indicated by the $Fe^{2+}/\Sigma Fe$ for a SME product assumed to be at 45 wt% total solids given the SRAT product analyses.

Table 7. Anion reaction extents in SRAT cycle, %

	NFT1-Rh	NFT2-Ru
Formate loss	15	16
Fe^{2+}/Fe total (post-run)	0.24	0.23

4.2 ELEMENTAL AND DISSOLUTION DATA

The two SRAT product samples were analyzed for bulk and supernate elements. The results of calculations on extent of elemental dissolution are given in Table 8.

Table 8. Extents of dissolution at the end of SRAT cycle, %

	Ca	Mg	Mn	Ni	Rh	Ru	S
NFT1-Rh	84	86	68	38	27	-	53
NFT2-Ru	83	76	66	30	-	1.8	42

Calcium dissolution extent remained near 80% as seen in several sets of recent SRAT products from different starting simulants. Magnesium extent of dissolution was about 81% which was lower than the ~100% expected. The moderately high Ni dissolution extent (compared to many tests where the extent is near zero) also seems to indicate conditions were favorable for 100% Mg dissolution. Manganese extent of dissolution was about 2/3rd of the total indicating either partial reduction or total reduction with partial re-precipitation. The extent of sulfur dissolution indicates potential formation of sulfate precipitates.

The bulk elemental composition of the calcined solids from the two SRAT product slurries calcined solids is given in Table 9.

Table 9. SRAT product calcined (1100 °C) elemental composition, wt%

Element	NFT1-Rh	NFT2-Ru
Al	6.75	6.66
Ba	0.227	0.220
Ca	3.15	3.03
Ce	0.224	0.222
Cr	0.268	0.267
Cu	0.096	0.124
Fe	23.4	23.7
K	<0.10	<0.10
La	0.136	0.127
Mg	2.10	2.13
Mn	9.45	9.53
Na	13.1	13.0
Ni	5.23	5.22
P	<0.10	<0.10
Pb	0.020	0.027
S	0.382	0.381
Si	0.680	0.711
Sn	0.098	0.097
Ti	0.021	0.021
Zn	0.212	0.210
Zr	0.206	0.217

Results for the two SRAT products were very similar as expected given the common starting sludge simulant.

4.3 PROBE DATA

Data on the pH of the SRAT slurry during processing were obtained in both runs. Data on the oxidation-reduction potential (ORP) of the SRAT supernate were obtained during the rhodium simulation. Data on pH profiles for the two runs are given in Figure 1.

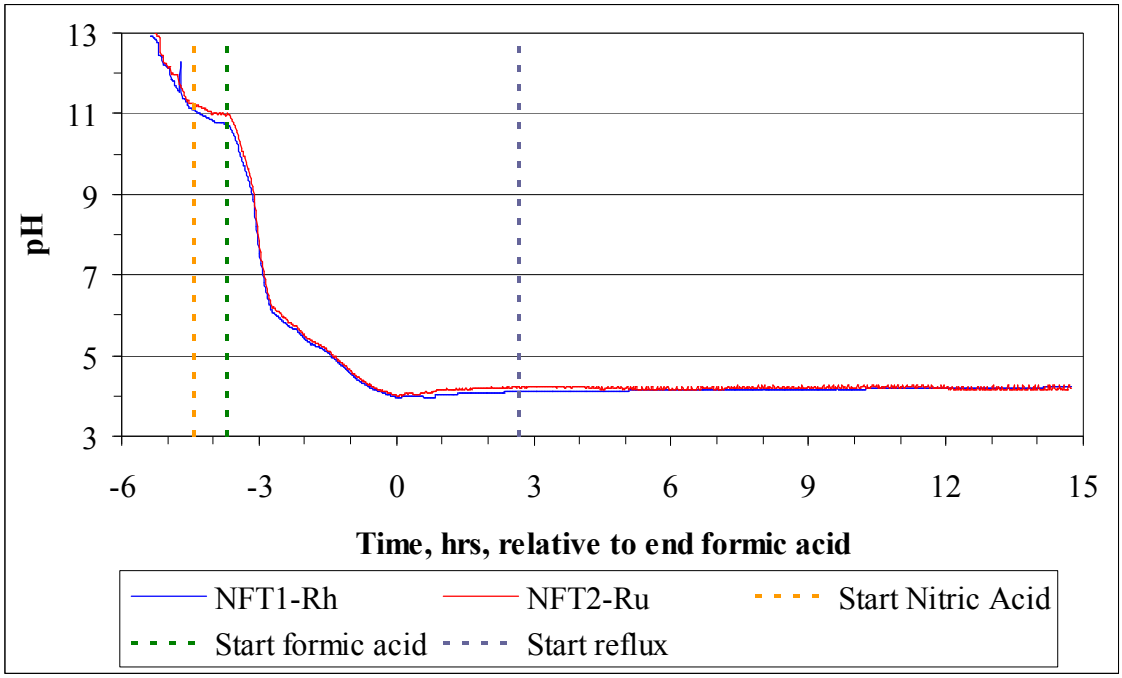

Figure 1. Nitrite-free simulant pH probe data

The two pH profiles were essentially identical suggesting that Rh and Ru were either both inactive (most likely) or that they did exactly the same thing in both simulations (unlikely). The lack of significant rise after acid addition indicates low catalytic activity and low formate destruction.

Both pH and ORP probe data were obtained on the rhodium run. The data are given in Figure 2. The ORP probe reading is in relative millivolts.

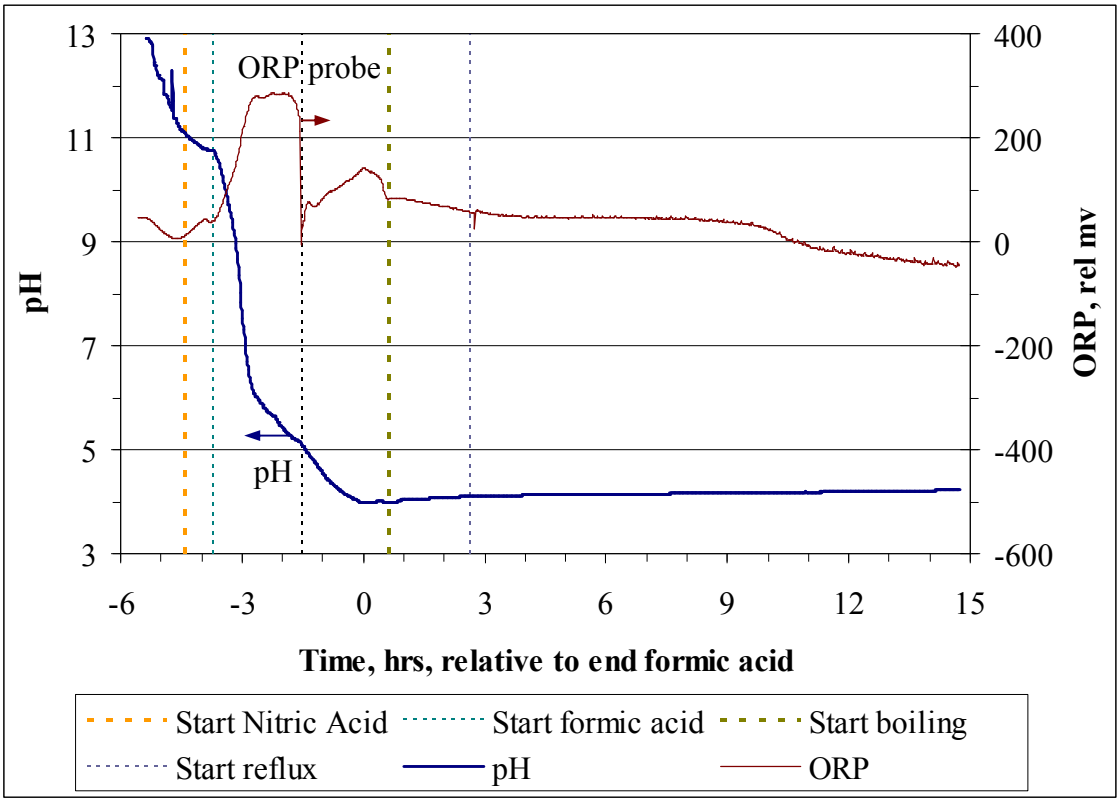

Figure 2. ORP and pH probe data for the Rh nitrite-free run

The ORP probe was checked against two "standard solutions". The nominal ORP potentials of the standard solutions are uncertain by ±10%. The ORP probe was reading high by 30-60 mV during the testing. One large ORP feature was seen during formic acid addition centered at about 2.5 hours before the end of formic acid addition. This was in contrast to a pair of comparably large features that were seen in two of the recent sludge matrix study runs, Figure 3.

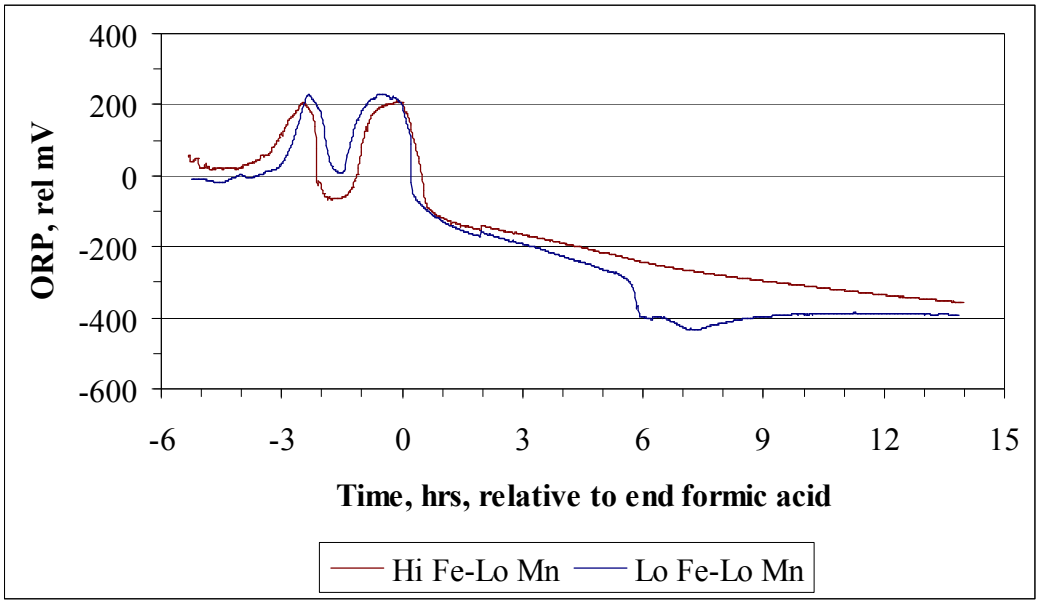

Figure 3. Sludge matrix study ORP data

The primary feature in the nitrite-free Rh run seemed to occur over roughly similar pH ranges to the first peak in the sludge matrix study runs. In particular, the initial feature in both runs came as the pH was dropping rapidly from nine into the acidic range.

There was a suggestion of a second feature in the nitrite-free run with a small peak at about a half hour before the end of formic acid addition, but it was much less pronounced than in the sludge matrix study. Nevertheless, the timing was comparable. This period is normally dominated by nitrite destruction reactions and manganese reduction. The sludge matrix study had these reactions occurring in parallel, while the nitrite-free run had only manganese reduction. That may offer a clue as to the interpretation of these features. ORP data will continue to be collected and the results correlated as future SRAT simulations are performed.

4.4 OFF-GAS DATA

GC data were obtained during both runs. The major finding from the GC data was the near total absence of any hydrogen generation in both tests. The run with Rh sporadically produced hydrogen just above the detection limit of the GC, while the run with Ru did not produce detectable hydrogen. The Rh data do not generate a smooth curve (the hydrogen peak went above and below the detection limit multiple times), so no graph is given. It is noteworthy that there was so little noble metal catalytic activity indicated in either run in the total absence of nitrite ion.

Peaks for NO and N_2O were not observed on the chromatographs of either run. No visual observations of any golden color in the off-gas were made. This was generally expected before the runs, but there was still the possibility that some nitrate ion might convert into nitrite and be destroyed producing these gases.

Data for CO_2 were fairly similar for the two runs, though not identical, Figure 4.

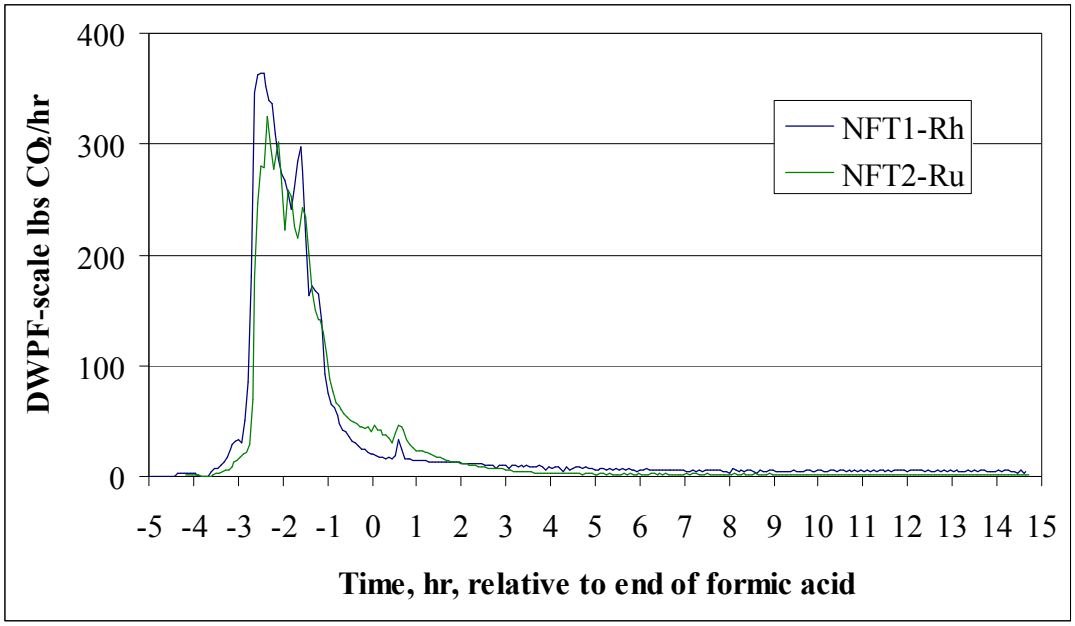

Figure 4. Carbon dioxide production at DWPF scale

The Rh run produced more CO_2 initially. The Ru run produced more CO_2 from -1 hour to +2 hours. The Rh run produced about 2.5 times as much CO_2 as the Ru run from +2 hours until the end of reflux. Reflux started at +2.7 hours, or after the time when the Rh went from lower to higher than the Ru run in CO_2 production rate. The post-acid addition GC data are expanded in Figure 5.

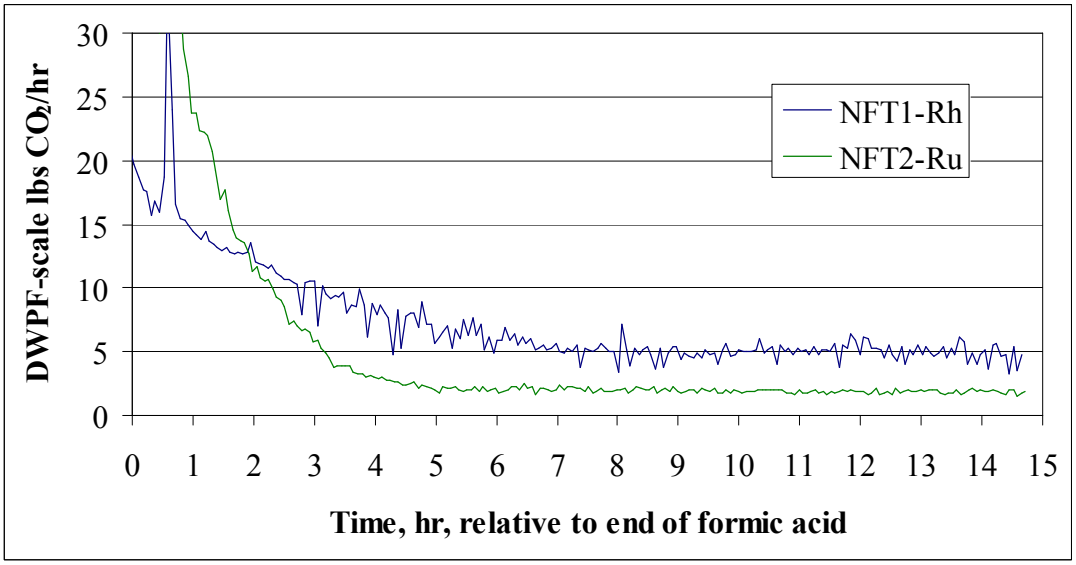

Figure 5. Carbon dioxide production after acid at DWPF scale

The greater CO_2 production rate during reflux in the Rh run compared to the Ru run may indicate some mild level of catalytic activity in the Rh run that was absent in the Ru run. This would be consistent with the trace quantities of hydrogen seen in the Rh run.

The Rh run produced 34.4 g of CO_2 versus 29.7 g in the Ru run. The Ru run number is the more uncertain of the two. The uncertainty was due to issues with the accuracy of the internal standard gas, He, area calibration factor. The helium peak was superimposed on a sloped baseline caused by an internal back flush feature in this particular GC that could not be disabled.

Destruction of carbonate, reduction of Hg, and reduction of about 67% of the Mn (per Table 8) should produce 11.0, 1.6, and 17.8 g of CO_2 respectively, or 30.4 g total which is consistent with the GC data. It also seems to imply that Mn reduction did not reach 100% at any intermediate point in the SRAT cycle, however, which is not the expected outcome of a SRAT run with significant excess acid and a sustained low pH.

The IC data for formate indicated a 31-32 g loss of formate (difference of formic acid in and the SRAT product formate out). If destroyed formate makes CO_2, then combining this with the carbonate destruction should have made 41.8 g of CO_2. This is 22% more than the Rh run result of 34.4 g and appears to be outside the likely range of random error for the integrated CO_2 total (GC calibrations held well during the runs and the He MKS flow controller is unlikely to be off by 20%, especially when it gives the proper vol% He when combined with purge air prior to starting the SRAT cycle). SRAT product formate mass was about 180 g, and this number could be uncertain by 10-20 g which would cover the difference with the GC data. Nevertheless, the two separate run results were nearly identical, and 30 g of formate loss is just enough to reduce all of the Hg and Mn that were present in the simulant.

One hypothesis that could reconcile the GC and IC data is that a fraction of the formate loss was either reabsorbed as insoluble carbonate or bicarbonate precipitate or was released as another gas. It was also noted that the ratio of O_2/N_2 increased during the main CO_2 peak (this region is normally obscured by O_2 consumption due to reaction with NO during tests with nitrite containing feeds). The ratio then returned to the normal range after the main CO_2 peak. Molecular oxygen is not a presumed byproduct of MnO_2 reduction. The presumed reaction is given by:

$$MnO_2 + 3HCOOH \rightarrow Mn(HCOO)_2 + CO_2 + H_2O$$

The observation about the O_2/N_2 ratio may or may not be related, but it could imply that some variation of the above chemistry was occurring. For example, conversion of Mn(IV) to Mn(III) instead of Mn(II) would be expected to produce half as much CO_2.

The GCs have been found to be able to detect the presence of water vapor in the off-gas. By adjusting the column injection interval, the water peak is generally kept out of the region of the B column where CO_2 and N_2O elute. The water peak is actually moving through the column very slowly, and the peak is usually from one injection earlier than the one producing

the CO_2 and N_2O peaks. The water peak area was used to monitor the impact of the Nafion dryer on the moisture content of the off-gas leaving the chilled condenser. Compressed air was fed through a Drier-Rite column and then fed counter-currently to the off-gas in the Nafion dryer. A ratio of five to one was used for the dried air flow to the SRAT purge air flow. The uncalibrated moisture content of the off-gas as a function of time is given in Figure 6 (units are microvolt-seconds, that is raw GC integration units).

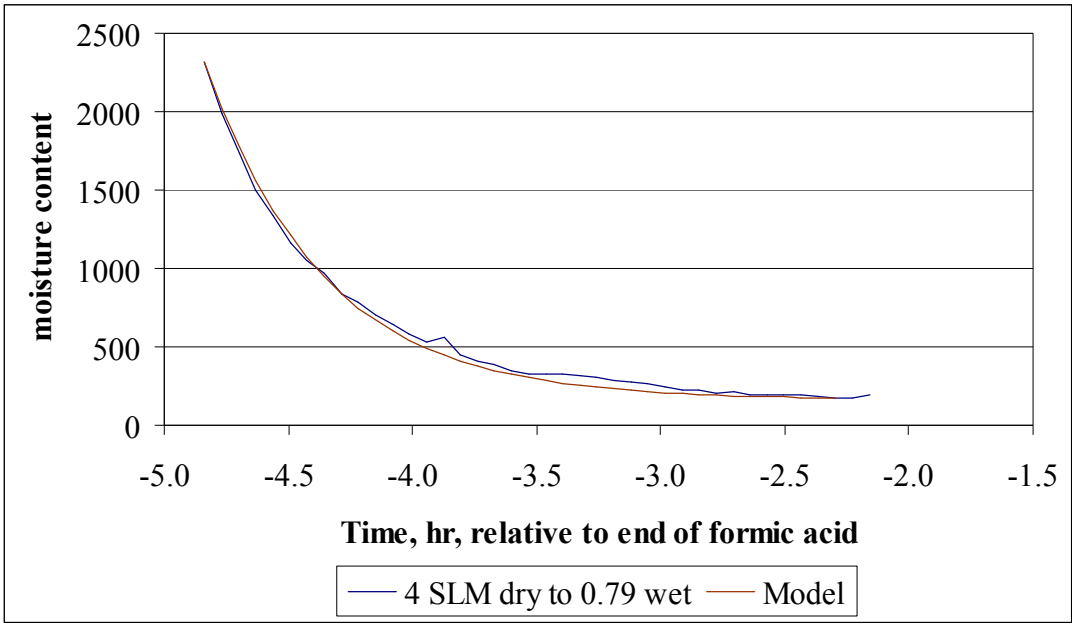

Figure 6. Off-gas moisture to GC as function of dryer time on-line

The model function contained an exponential decay function with a pre-exponential factor, exponent multiplier constant for time, and an additive constant.

$$moisture\ content = 2166e^{-2.1*delta\ t} + 163$$

where *delta t* was the elapsed time from the start of drying. A 92% reduction in the moisture content of the chilled air coming out of the 4 °C condenser was achieved after about two hours. The additive constant, 163, may or may not approximate the moisture content of the dry air purge, but in any case, it is not expected that the dryer could reduce the moisture content of the chilled off-gas air below the moisture content of the dry air purge. It is thought that reducing the moisture content of the gas injected into the GCs will prolong their service life due to reduced corrosion attack from nitric and nitrous acids. Data were not obtained for NFT2, since the water peak fell outside the recorded period of the chromatographs (3 minutes of data are recorded out of a 4.5 minute sampling cycle).

4.5 DATA IMPLICATIONS FOR CATALYTIC HYDROGEN GENERATION

As discussed in the catalytic hydrogen generation status report, a growing body of evidence had been accumulated that tended to support the concept of a nitro-Rh complex as the

primary active form of rhodium for hydrogen production.[1] Rhodium-based production of hydrogen was detected at low nitrite ion concentrations near the end of nitrite destruction. The primary peak due to rhodium seemed to end as nitrite destruction went to completion. Residual catalytic activity of rhodium existed, but the form of the active species was unknown. The new data from the nitrite-free Rh test fully support these preliminary conclusions and hypotheses about the mechanism of catalytic rhodium driven hydrogen generation. It may even be necessary for rhodium to pass through the nitro-Rh complex stages before it can transition into a less active form. The current test did not appear to ever form a nitrite ligand-free less active form.

Less was known about catalytic hydrogen generation by Ru prior to the nitrite-free Ru test. The new data do not alter the conclusions in the summary status report.[1] The total lack of hydrogen production, however, was not anticipated. The earlier data indicated that Ru became catalytically active once nitrite was essentially destroyed. In the absence of nitrite ion, it was assumed that Ru might become catalytically active immediately, or at least once a certain pH range was reached where Ru solubility combined with the presence of excess acid would lead to hydrogen generation. It had been postulated that a nitro-Ru complex may have been preventing hydrogen generation prior to nearly complete nitrite destruction in earlier tests. A new hypothesis can be made that a nitro-Ru complex is a necessary precursor to the catalytically active form of Ru for hydrogen generation. Consequently, by never forming the nitro-Ru complex in the nitrite-free SRAT run, the catalytically active form never had a chance to form.

5.0 CONCLUSIONS

Two SRAT simulations were completed using a nitrite-free starting simulant, one with Rh and Hg and the other with Ru and Hg. Noble metals were trimmed at the high end of the recent Rh-Ru-Hg study. Mercury was trimmed at 1.5 wt% in the total solids. Excess acid comparable in quantity to that in the recent Rh-Ru-Hg matrix study was used. In spite of the favorable conditions for hydrogen generation, virtually no hydrogen production was observed during either SRAT simulation.

The Rh test result confirms the postulated significance of nitrite ion to the catalytic reactions producing hydrogen in CPC testing with normal SRS simulants. As for Ru, however, previous testing has shown that Ru activated for hydrogen generation only after nitrite destruction. Therefore, Ru could have potentially been catalytically active for hydrogen production from the start of the nitrite-free SRAT test but no such activity was seen. The Ru test result suggests that the intermediate Ru form detected in the bead-frit melter feed preparation noble metal solubility profiles was some form of nitro-Ru complex. The nitro-Ru complex is apparently not catalytically active for hydrogen generation but is a precursor to the catalytically active form (presumably a different complex not involving nitrite ligands). Removing nitrite ion from the system prevented the Ru catalyst precursor from forming and consequently prevented the catalytically active form.

The new data add to the overall fundamental understanding of catalytic hydrogen generation during SRS waste processing in the DWPF. When combined with results from an earlier SRAT simulation in which sodium nitrite was metered into the vessel to inhibit ligand substitution reactions and hydrogen generation, the new findings have greatly clarified the role of the nitrite ion in catalytic SRAT hydrogen generation reactions. These findings address one of the issues related to nitrite ion raised in the Future Work section of the recent summary document concerning catalytic hydrogen generation in the CPC.[1]

6.0 ACKNOWLEDGMENTS

I would like to acknowledge the assistance of M. F. Williams in preparing the GC's for operation during these tests. The GC data were critical to any evaluation of catalytic hydrogen generation. Method development was required to deal with the internal back flush on one of the GCs to reach a point where post-run reprocessing could extract reasonable values for the internal standard concentration (helium). I would also like to acknowledge the work of J. W. DuVall and D. P. Healy in preparing the nitrite-free simulant, and their assistance, along with V. J. Williams, I. A. Reamer, and T. O. Burckhalter in completing the SRAT simulations. I also wish to thank D. R. Best, P. Simmons, and W. T. Riley for the majority of the sample analyses.

7.0 REFERENCES

[1] Koopman, D. C., *DWPF Catalytic Hydrogen Generation Program – Review of Current Status*, SRNL-STI-2009-00214, SRNL, Aiken, SC, 29808 (July 2009).

[2] Lambert, D. P., B. R. Pickenheim, and D. R. Best, *DWPF SB6 Initial CPC Flowsheet Testing – SB6-1 to SB6-6 4L Tests of SB6-A and SB6-B Simulants*, SRNL-STI-2009-00413, SRNL, Aiken, SC, 29808 (July 2009).

[3] Koopman, D. C., *Statistical Evaluation of Processing Data from the Rh-Ru-Hg Matrix Study*, SRNL-STI-2009-00084, SRNL, Aiken, SC, 29808 (April 2009).

[4] Koopman, D. C., *Preliminary Evaluations of Two Proposed Stoichiometric Acid Equations*, SRNL-L3100-2009-00146, SRNL, Aiken, SC, 29808 (June 2009).

[5] Jantzen, C. M. and M. E. Stone, *Role of Manganese Reduction/Oxidation (RedOx) on Foaming and Melt Rate in High Level Waste Melters*, WSRC-STI-2006-00066, Savannah River National Laboratory, Aiken, SC, 29808 (March 2007).

Distribution:

S. L. Marra, 773-A
A. B. Barnes, 999-W
D. A. Crowley, 773-43A
S. D. Fink, 773-A
B. J. Giddings, 786-5A
C. C. Herman, 999-W
F. M. Pennebaker, 773-42A
J. E. Occhipinti, 704-S
D. C. Sherburne, 704-S
R. T. McNew, 704-27S
J. F. Iaukea, 704-30S
J. W. Ray, 704-S
H. B. Shah, 766-H
J. M. Gillam, 766-H
B. A. Hamm, 766-H
D. D. Larsen, 766-H
C. J. Bannochie, 773-42A
D. K. Peeler, 999-W
N. E. Bibler, 773-A
M. E. Stone, 999-W
B. R. Pickenheim, 999-W
J. D. Newell, 999-W
A. I. Fernandez, 999-W
J. M. Pareizs, 773-A
S. H. Reboul, 773-A
J. M. Bricker, 704-27S
T. L. Fellinger, 704-26S
E. W. Holtzscheiter, 704-15S
M. T. Keefer, 766-H